Cooperative Behaviors in Carbene Additions through Local Modifications of Nanotube Surfaces

Takashi Yumura*,†,‡ and Miklos Kertesz*,†

Department of Chemistry, Georgetown University, 37th and O streets NW, Washington, DC, 20057-1227, and Department of Materials Science and Engineering, Meijo University, Tenpaku-ku, Nagoya 468-8502, Japan

Received September 27, 2006. Revised Manuscript Received December 6, 2006

We investigate the cooperative behavior of two carbene additions to a (5,5) armchair single-walled carbon nanotube (SWNT) and find that in certain configurations, double additions are more stable than uncorrelated distant double additions by 7 to 24 kcal/mol. We also find certain configurations to be very unstable. We employ density functional theory (DFT) PW91 calculations using periodic boundary conditions and compare 20 different double-addition configurations. We trace the cooperative behavior to the power of the first addition to modify the geometry locally. We investigate both inner (endohedral) and outer (exohedral) additions and observe fundamental differences between these two. In the qualitative interpretations of the results, analogies to the valence tautomerization of 1,6-methano[10]annulene are helpful in establishing that when the carbene addition opens the CC bond in the nanotube (exohedral addition), then the number of π-electrons is unchanged, leading to less spatially extended perturbations of the nanotube. Endohedral carbene additions reduce the number of π-electrons, leading to a more pronounced and spatially more extended cooperative effect. We find that local quinonoid-like perturbations of the geometry extend over several rings near the endohedral perturbation. Such extended defects should play a role in the properties of substituted nanotubes and can be visualized using Clar diagrams.

Introduction

Single-walled carbon nanotubes (SWNTs)[1] exhibit a metallic or semiconducting character, depending on their chirality (*n*,*m*), due to the delocalized π-electrons of the sp^2 hybridized carbon atoms forming a hexagonal network. Their interesting properties can be modified by chemical functionalization in which covalent bonds are formed between adsorbents and the nanotube.[2] Up to now, SWNT surfaces have been reported to bind covalently with highly reactive reagents.[2] For example, Haddon et al. reported that SWNTs treated by nitric acid were successfully functionalized by divalent carbenes.[3−5] The binding of carbenes into the SWNT surfaces has been analyzed by density functional theory (DFT) calculations.[6−11] Zhao et al. found that the metallic character of armchair nanotubes will be retained at low levels of carbene functionalization.[9] DFT calculations on conductance of the carbene-functionalized SWNTs with random configurations indicate that the functionalization reduces but does not eliminate the conductance.[10,11]

Although the physical properties of functionalized nanotubes have been discussed, the geometrical changes on the surface, which should be sensitive to the additions, remained relatively unexplored. The disruption of the π systems, created by the addition of the first carbene, should induce formation of addition patterns with possible preferential sites for subsequent additions of carbenes. In fact, addition patterns of SWNTs functionalized by the the Bingel reaction have been analyzed by atomic force microscopy (AFM)[12] and scanning tunneling microscopy (STM).[13] In particular, Kruse et al. proposed from STM observations that long-range (several nanometer) periodicities of the addition patterns on the functionalized SWNTs.[13] Understanding on a molecular scale how disruptions of the π systems by carbenes ties in with the formation of addition patterns on nanotube surfaces is promising for establishing strategies for constructing "tailor-made materials" based on nanotubes.

Recent transmission electron microscopy (TEM) observations[14,15] and density functional theory (DFT) calculations[16,17] on defected nanopeapods, in which defected fullerene

* Corresponding author. E-mail: yumura@ccmfs.meijo-u.ac.jp (T.Y.) and kertesz@georgetown.edu (M.K.).
† Georgetown University.
‡ Meijo University.

(1) Iijima, S.; Ichihashi, T. *Nature* **1993**, *363*, 603.
(2) Hirsch, A. *Angew Chem., Int. Ed.* **2002**, *41*, 1853.
(3) Chen, J.; Hamon, M. A.; Hu, H.; Chen, Y.; Rao, A. M.; Eklund, P. C.; Haddon, R. C. *Science* **1998**, *282*, 95.
(4) Hu, H.; Zhao, B.; Hamon, M. A.; Kamaras, K.; Itkis, M. E.; Haddon, R. C. *J. Am. Chem. Soc.* **2003**, *125*, 14893.
(5) Kamaras, K.; Itkis, M. E.; Hu, H.; Zhao, B.; Haddon, R. C. *Science* **2003**, *301*, 1501.
(6) Chen, Z.; Nagase, S.; Hirsch, A.; Haddon, R. C.; Thiel, W.; Schleyer, P. v. R. *Angew. Chem., Int. Ed.* **2004**, *43*, 1552.
(7) Bettinger, H. F. *Org. Lett.* **2004**, *6*, 731.
(8) Bettinger, H. F. *Chem.—Eur. J.* **2006**, *12*, 4372.
(9) Zhao, J.; Chen, Z.; Zhou, Z.; Park, H.; Schleyer, P. v. R.; Lu, J. P. *ChemPhysChem* **2005**, *6*, 598.
(10) Park, H.; Zhao, J.; Lu, J. P. *Nano Lett.* **2006**, *6*, 916.
(11) Lee, Y.-S.; Marzari, N. *Phys. Rev. Lett.* **2006**, *97*, 116801.
(12) Coleman, K. S.; Bailey, S. R.; Fogden, S.; Green, M. L. H. *J. Am. Chem. Soc.* **2003**, *125*, 8722.
(13) Worsley, K. A.; Moonoosawmy, K. R.; Kruse, P. *Nano. Lett.* **2004**, *4*, 1541.
(14) Urita, K.; Sato, Y.; Suenaga, K.; Gloter, A.; Hashimoto, A.; Ishida, M.; Shimada, T.; Shinohara, H.; Iijima, S. *Nano Lett.* **2004**, *4*, 2451.
(15) Sato, Y.; Yumura, T.; Urita, K.; Suenaga, K.; Kataura, H.; Kodama, T.; Shinohara, H.; Iijima, S. *Phys. Rev. B.* **2006**, *73*, 233409.

10.1021/cm0623108 CCC: $37.00
Published on Web 02/10/2007

molecules are encapsulated inside SWNTs, would provide helpful hints to make some realistic progress in this direction. In a previous study, DFT calculations demonstrate that the nanotube surface is locally modified by the bond formation with a defected fullerene, with a single C atom protruding from the fullerene.[17] The TEM observations have also detected the bond formations and concomitant surface deformations.[14] Such local deformations can result from interactions of the surface with "inner" carbene molecules, or defected fullerenes. In the present paper, we will discuss the effects of local modifications of nanotube surfaces on site preferences for the addition of a second CH_2 using DFT calculations. We discuss two issues: the disruptions of CC bonding networks by the addition of the first CH_2 molecule into the outer or inner SWNT surface, and the energetics for the second CH_2 addition.

Method of Calculation

We carried out DFT calculations on the basis of the generalized gradient approximation Perdew−Wang (PW91) functional.[18] The calculations for the (5,5) armchair nanotube were performed using the Vienna ab initio Simulation Package (VASP v.4.4.5).[19,20] The kinetic energy cutoff of the plane-wave basis is 349 eV with ultrasoft Vanderbilt-type pseudopotentials. In this study, a hexagonal supercell is used, containing 80 C atoms of the (5,5) nanotube and one or two CH_2 molecules to avoid interactions between CH_2 groups located on the neighboring unit cells. We allow full geometry relaxation, except that we fixed the intertube distance at 6 Å, which is large enough to avoid significant intertube interactions.[20] We used a $1 \times 1 \times 15$ *k*-point mesh for all geometry optimizations.[21] Convergence was enhanced using fractional occupancy generated by a Gaussian broadening ($\sigma_{GB} = 0.03$ eV) of the one-electron energy levels. To analyze size effects for the double CH_2 additions,[22] we calculated the finite-length armchair (5,5) $C_{140}H_{20}$ systems using the PW91PW91 functional with the 6-31G* basis set in the Gaussian 03 program.[23]

Results and Discussion

We will discuss the addition of the carbene molecule, as shown in Scheme 1, into inner and outer surfaces of the nanotubes for the following reasons. In comparisons between the endohedral and exohedral additions, it is interesting to investigate chemical reactivities on convex and concave surfaces. Furthermore, local modifications on the surface due to interactions of an inner CH_2 molecule should be analogous to the defected nanopeapods, and should play an important role in site-selective additions. Up to now, various types of

Scheme 1

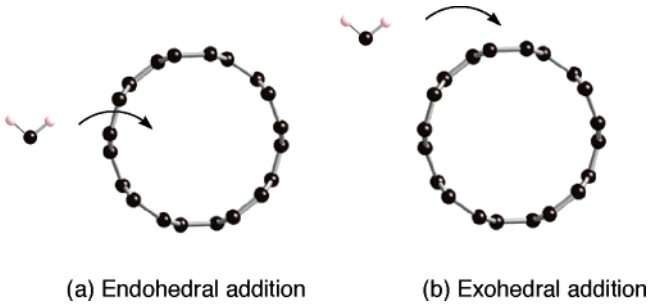

molecules, such as fullerenes,[24,25] *o*-carbonane,[24] hydrocarbons,[24] water,[26] metal complexes,[24] and I_2,[27] have been reported to be encapsulated in uncapped nanotubes. According to ref 25, nanopeapods can be simply prepared in the liquid phase. The widely applicable liquid preparations allow us to incorporate various guest molecules into nanotubes, if appropriate solvents can be found.[25] Thus, we consider the possibility that the precursors for free carbene molecules[28] can enter into nanotubes, which should stimulate experimental efforts. Once the precursors enter the nanotubes, carbene molecules, generated from the inner precursors,[28] should attack inner surfaces rather than outer surfaces.

As shown in Figure 1, there are two optimized geometries for the addition of the CH_2 molecule into each surface, because the armchair nanotube has two types of CC bonds (CC bonds orthogonal (**O**) and slanted (**S**) relative to the tube axis, see Chart 1). One optimized geometry has the CH_2 molecule binding into an orthogonal CC bond (**O**) on the inner surface, and the other has the CH_2 molecule binding into a slanted CC bond (**S**). In both optimized geometries **O** and **S**, the CH_2 molecule binds into the surface to form two CC bonds of ∼1.54 Å, and a three-membered ring results. The additions into the inner surface of the SWNT are exothermic, as shown in Table 1, where binding energies are defined as $E_{B.E.}^{first} = E(CH_2{-}SWNT) - E(SWNT) - E(CH_2)$, where $CH_2{-}SWNT$ indicates optimized geometries for the functionalized SWNT after the first addition. Table 1 also shows that the orthogonal binding inside the nanotube is preferable to the slanted site by 12.3 kcal/mol. Site preferences in the exohedral additions are even more significant; the optimized structure **O** is more stable than the optimized geometry **S** by 29.7 kcal/mol, consistent with Bettinger's results.[8] The stabilization energies in the exohedral additions are larger than those in the endohedral additions. These data suggest that the outer surface should

(16) Yumura, T.; Sato, Y.; Suenaga, K.; Urita, K.; Iijima, S. *Nano Lett.* **2006**, *6*, 1389.
(17) Yumura, T; Kertesz, M.; Iijima, S. *J. Phys. Chem.* **2007**, *111*, 1099.
(18) Perdew, J. P.; Wang, Y. *Phys. Rev. B* **1992**, *45*, 13244.
(19) Kresse, G.; Furthmüller, J. *Phys. Rev. B* **1996**, *54*, 11169.
(20) The VASP code has been validated for structures of various organic molecules, conjugated molecules, graphite, diamond, and carbon nanotubes. Sun, G.; Kürti, J.; Kertesz, M.; Baughman, R. H. *J. Am. Chem. Soc.* **2002**, *124*, 15076.
(21) We investigated convergency of the total energy for a (5,5) nanotube system with two attached CH_2 groups with various $1 \times 1 \times nk$ *k*-point meshes (with $nk = 4$, 10, 15, 20, 25, 30). We confirmed that the total energy is converged with $nk = 15$.
(22) Yumura, T.; Bandow, S.; Yoshizawa, K.; Iijima, S. *J. Phys. Chem. B* **2004**, *108*, 11426.
(23) Frisch, M. J.; et al. *Gaussian 03*; Gaussian, Inc.: Pittsburgh, PA, 2003.
(24) Khlobystov, A. N.; Britz, D. A.; Briggs, G. A. D. *Acc. Chem. Res.* **2005**, *38*, 901.
(25) Yudasaka, M.; Ajima, K.; Suenega, K.; Ichihashi, T.; Hashimoto, A.; Iijima, S. *Chem. Phys. Lett.* **2003**, *380*, 42.
(26) Maniwa, Y.; Kataura, H.; Abe, M.; Suzuki, S.; Achiba, Y.; Kira, H.; Matsuda, K. *J. Phys. Soc. Jpn.* **2002**, *17*, 2863.
(27) Kissel, K. R.; Hartman, K. B.; Van der Heide, P. A. W.; Wilson, L. J. *J. Phys. Chem. B* **2006**, *110*, 17425−17429.
(28) In refs 3−5, $PhHgCCl_2Br$ dissolved in dichlorobenzene was used as a precursor for free CCl_2, and the functionalization was performed by heating the precursors at 85 °C. A possible candidate for a precursor to free CH_2 is diazomethane CH_2N_2. In fact, C_{60} fullerene molecules were functionalized using decompositions of CH_2N_2 dissolved in toluene by heating (thermolysis) or irradiating with light (photolysis). Diederich, F.; Thilgen, C. *Science* **1996**, *271*, 317.

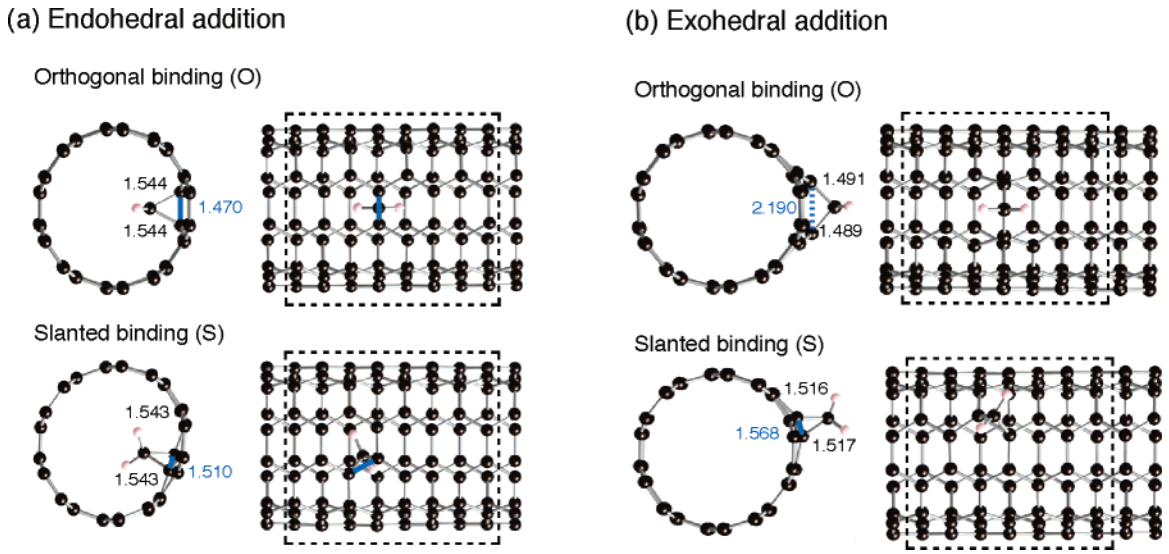

Figure 1. Two optimized geometries for the addition of the CH_2 molecule into the (a) inner and (b) outer surfaces of the (5,5) nanotube. In the top two cases, the CH_2 groups are attached to a CC bond orthogonal to the tube axis (**O**); in the bottom two cases, the CH_2 groups are attached to a CC bond slanted to the tube axis (**S**). The binding sites are in blue.

Chart 1

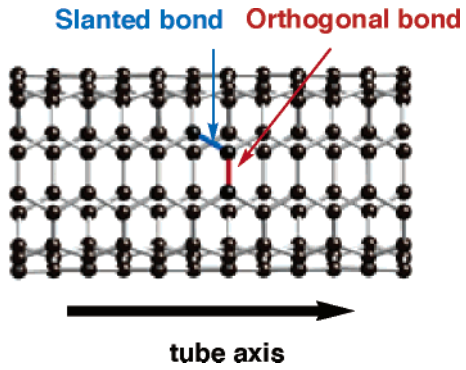

Table 1. Binding Energies in kcal/mol for the Addition of the CH_2 Molecule into the Outer or Inner Surface of the (5,5) Nanotube.[a]

	endohedral addition		exohedral addition	
	orthogonal (O)[b]	slanted (S)[b]	orthogonal (O)[b]	slanted (S)[b]
$E_{B.E.}^{first}$[c] (kcal/mol)	−44.7	−32.4	−117.0	−87.3
$d_{1,6}$ (Å)	1.470	1.510	2.190	1.568
$d_{1,6}$ (Å)[d]			2.15−2.26	∼1.57

[a] The optimized lengths (Å) of the C═C bond on the surface, into which the CH_2 molecule binds, are also given as $d_{1,6}$. For a definition of $d_{1,6}$, see Scheme 2. The bond reported corresponds to the bond to which CH_2 is attached. [b] O and S refer to the binding orientations of $d_{1,6}$ relative to the tube axis, as illustrated in Chart 1. [c] $E_{B.E.}^{first} = E(CH_2{-}SWNT) - E(SWNT) - E(CH_2)$. [d] From ref 8; periodic boundary condition calculations were employed using a gradient corrected functional (PWE/3-21G).

be more reactive than the inner surface, similar to those in monovalent F or H atom addition.[29] In exohedral additions, their binding structures depend on the sites where the CH_2 molecule attacks in Figure 1; the optimized structure **O** has the CH_2 molecule cleaving the orthogonal CC bond (insertion-type), whereas the optimized structure **S** has a three-membered ring. The two optimized geometries in the exohedral additions are in agreement with those obtained from previous DFT studies (Table 1).[6−11]

Scheme 2

1,6-methano[10]annulene

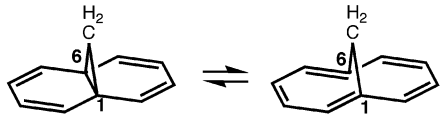

bisnorcaradiene form 1 **aromatic form 2**

Carbene addition into the nanotube surface is related to carbene addition into the C1C6 bridgehead of naphthalene,[30] where the valence tautomerism of 1,6-methano[10]annulene occurs, as shown in Scheme 2. With respect to the tautomerization, long distances of $d_{1,6}$ are preferable in the tautomerization of 1,6-methano[10]annulene.[31] As shown in Figure S1 of the Supporting Information, these results can be well-reproduced at the PW91 calculations; the optimized $d_{1,6}$ value is 2.291 Å.[31] On the nanotube surface, the convex and concave shapes should affect this bond. In the exohedral addition, the binding of the CH_2 molecule into the orthogonal CC bond splits this CC bond, whereas in the slanted case, it does not. Since the optimized geometry **O** is more stable in energy than the optimized geometry **S**, the exohedral additions exhibit a trend similar to that of the addition into naphthalene in terms of relationships between its stabilities and $d_{1,6}$ values. In the endohedral additions, opposite trends are seen; the orthogonal CC binding is preferable relative to the slanted CC binding, although the length of the orthogonal bond (1.479 Å) is shorter that in the slanted bond (1.531 Å). The difference between the exohedral and endohedral additions can be rationalized by a strain analysis using a π-orbital axial vector (POAV) in which the strain energy is

(29) Chen, Z.; Thiel, W.; Hirsch, A. *ChemPhysChem* **2003**, *1*, 93.
(30) Vogel, E.; Roth, H. D. *Angew. Chem., Int. Ed.* **1964**, *3*, 228.
(31) The optimized $d_{1,6}$ values depend significantly on substitutions in derivatives of 1,6-methano[10]annulene; Choi, C. H.; Kertesz, M. *J. Phys. Chem. A* **1998**, *102*, 3429. The optimized $d_{1,6}$ value is consistent with that obtained experimentally (2.235 Å). The consistency indicates reliability of our choice of the PW91 DFT calculations; Bianchi, R.; Pilati, T.; Simonetta, M. *Acta Crystallogr., Sect. B* **1980**, *36*, 3147.
(32) Haddon, R. C. *J. Comp. Chem.* **1998**, *19*, 139.

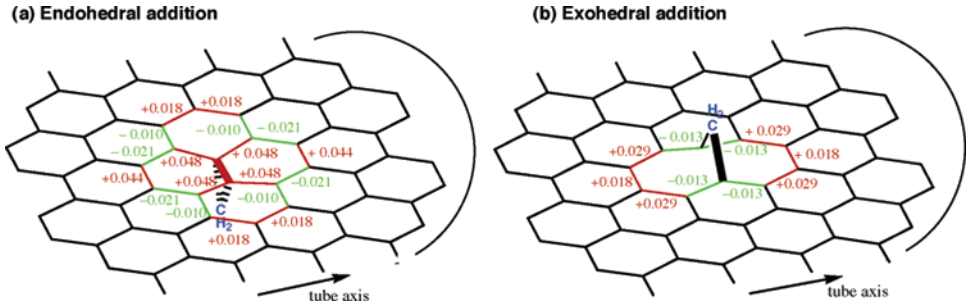

Figure 2. Deviations of CC bond lengths due to the binding of the CH_2 molecule into an orthogonal CC bond. (a) Endohedral and (b) exohedral addition. Red and green lines indicate a CC bond whose length increases or decreases by at least 0.01 Å, respectively, relative to those in the pristine nanotube. Semicircles on the right indicate the wrapping of the sheet into a nanotube.

proportional to the square of a POAV pyramidal angle:[32] in the exohedral addition where the $d_{1,6}$ CC bond cleaves, POAV values in the C atoms where the CH_2 molecule attaches decrease and therefore strains of the (5,5) nanotube are partially relaxed, whereas in the endohedral additions, such strain relaxations cannot occur because of the more rigorous restrictions of surface relaxations toward the tube axis. The different $d_{1,6}$ values play a crucial role in the disruptions of the π-systems on the nanotube surface.

Next, we focus on the changes of CC bonding on the nanotube surface in the orthogonal CC additions, which are more favorable than the slanted additions. Figure 2 shows the CC bonds on the surface, whose lengths increase or decrease at least by 0.01 Å upon the carbene addition, which are given by red or green, respectively. As shown in Figure 2a, the carbon network is locally perturbed near the binding site. In endohedral addition, the locally perturbed network has bisnorcaradiene-like moieties on the two hexagons nearest to the binding site in the axial direction. We can see also in Figure 2a bond-length alternation with substantial decreases in orthogonal CC bonds and increases in slanted CC bonds in the two hexagonal rings nearest to the binding site in the circumferential direction. Such perturbations on the surface by the exohedral addition are limited to the axial direction; the four CC bonds nearest to the binding site are shortened by ~0.01 Å. The deviations in the lengths in the inner addition (−0.012 to +0.029 Å) are significantly smaller relative to those in the outer addition (−0.022 ~ +0.048 Å).

Simple "Clar" valence bond (VB) representations can be used to aid the qualitative interpretation of the disruptions of the π-systems on the SWNT surface.[33] All π-electrons of armchair nanotubes can be assigned to "aromatic sextets", as proposed by Matsuo et al.[34] and Ormsby et al.[35] As mentioned above, DFT calculations show that the endohedral CH_2 addition retains the C1C6 bond on the surface, whereas the exohedral addition splits the C1C6 bond. These observations indicate that two π-electrons are removed from the surface in the endohedral addition to form the new σ-bonds, whereas in the exohedral addition, two σ-electrons migrate to form the new σ-CC bond, accompanied by a rotation but not removal of two π-electrons from the surface. Taking this important π-electron count difference into account, we consider the CC bonding networks upon the inner and outer additions. Three representations B_1(in), B_2(in), and Q(in) (K_1(out), K_2(out), and C(out)) can qualitatively help interpretation of the optimized geometries for the endohedral (exohedral) addition, as shown in Figure 3, where aromatic sextets are represented by circles. Because of the binding into the surface, butadiene-like patterns are formed in the B_1(in) and B_2(in) frameworks and a quinonoid pattern is formed in the Q(in) framework, as shown in Figure 3. The local modifications of the bisnorcaradiene-like framework obtained from DFT calculations correspond to the combination of the degenerate B_1(in) and B_2(in), and the bond-length alternation in the circumferential direction corresponds to a part of the quinonoid framework Q(in). This bond-length alternation in the circumferential direction, associated with the Q(in) framework, is plotted in Figure 4, which is only significant near the binding site. In contrast to the endohedral addition, deformations due to the exohedral addition are limited to the two hexagon rings nearest to the binding site along the tube axis; the K_1(out) and K_2(out) representations have Kekulé-like patterns near the binding site and the C(out) representation retains the Clar patterns of the unperturbed nanotube. Thus, the endohedral addition significantly perturbs π-systems on the surface, in contrast to the carbon network in the exohedral addition case, where the bonds of the network remain almost unchanged relative to those in the pristine nanotube, except in the immediate vicinity of the CH_2 binding. These findings are also useful in terms of the conductance of functionalized SWNTs, because these representations can provide qualitative information on the disruptions of conjugated networks. Marzari et al. reported that the conductance of nanotubes functionalized by carbene derivatives is preserved at high concentrations, whenever the functionalization breaks the $d_{1,6}$ CC bond.[11,36] Their predictions are in qualitative agreement with our findings for the following reasons; in nanotubes with the $d_{1,6}$ cleavage, the number of π-electrons is unchanged and their surfaces retain Clar networks, whereas in nanotubes without the $d_{1,6}$ cleavage, the number of π-electrons decreases and their Clar structures are disturbed because of the local quinonoid and bisnorcaradiene-like perturbations. When the CC bond at the attachment site is cleaved, one would expect this to be a larger perturbation of the hexagonal π-network than attachments that maintain the CC bond. The overall behavior is

(33) Clar, E. *The Aromatic Sextet*; Wiley: London, 1972.
(34) Matsuo, Y.; Tahara, K.; Nakamura, E. *Org. Lett.* **2003**, *5*, 3181.
(35) Ormsby, J. L.; King, B. T. *J. Org. Chem.* **2004**, *69*, 4287.
(36) Lee, Y.-S.; Nardelli, M. B.; Marzari, N. *Phys. Rev. Lett.* **2005**, *95*, 076804.

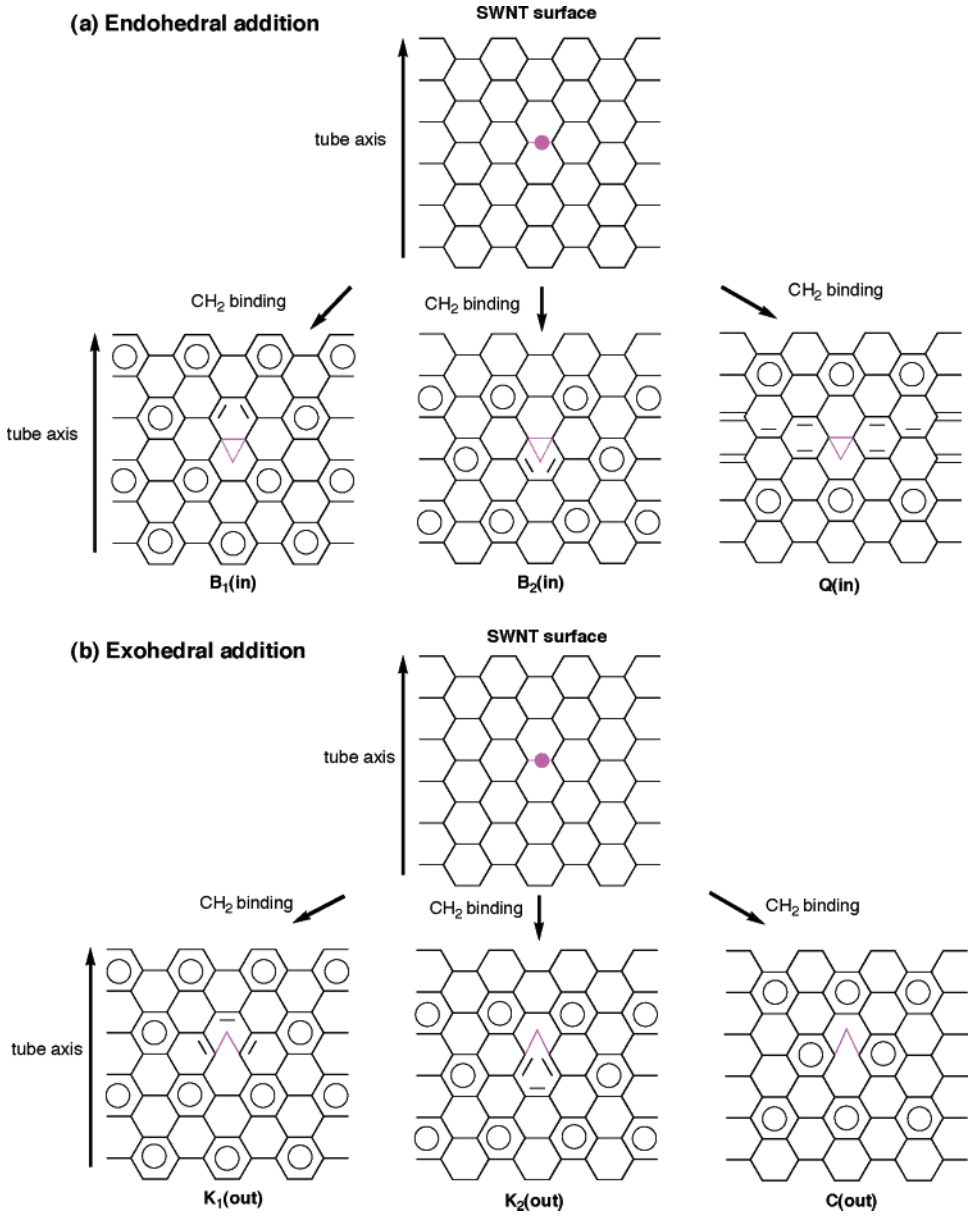

Figure 3. Clar valence bond (VB) representations for the addition of the CH_2 molecule into a orthogonal CC bond on the (a) inner and (b) outer nanotube surfaces. The purple dots represent binding sites for the CH_2 molecule. Aromatic sextets are indicated by circles. The tubes are presented as planar projections; only the vicinity of the addition site is shown.

therefore counterintuitive; however, it can be understood qualitatively by Clar valence bond (VB) representations.

Next, we discuss the effects of the local geometrical changes, created by the first addition, on the site preferences for the second CH_2 attachment. We will assume that the first CH_2 molecule binds into an orthogonal CC bond on the inner surface of the SWNT (Scheme 3), because the deviations caused by the inner addition are larger than those in the outer addition. Another advantage of this choice is that we can directly estimate effects of the local modifications on the site preferences without considering steric effects between the two CH_2 molecules. Taking the surface modifications in Figure 3 into account, we consider 20 sites for the binding of the second CH_2 molecule (Figure 5a). We define an orthogonal binding site for the second CH_2 molecule (outer surface) as $O_p(q)$ relative to the binding site $O_0(0)$ for the first CH_2 molecule (inner surface). Here p represents the order of the carbon belt of the $O_p(q)$ site, lying in a plane perpendicular to the axis, from the $O_0(0)$ site with respect to the armchair framework in the axial direction, and q represents the order of the orthogonal bond $O_p(q)$ with respect to the $O_0(0)$ site in the circumferential direction. In slanted binding sites, the $S_{p1-p2}(q)$ sites are between the p_{1st} and p_{2nd} carbon belts.

Figure 5b shows binding energies for the second additions ($E_{B.E.}^{second} = E(CH_2{-}SWNT{-}CH_2) - E(SWNT) - 2E(CH_2)$) as a function of the separation between the first and second binding sites projected upon graphene, where $CH_2{-}SWNT{-}CH_2$ indicates optimized geometries for the tube with two CH_2 units added. As shown in Figure 5b, where orthogonal (slanted) binding energies are shown in blue (purple), all second CH_2 additions are exothermic, and orthogonal additions are energetically more favorable than slanted additions. This trend is similar to that of the first attachment. Figure 5b shows that the binding energies for the orthogonal and slanted additions have nearly constant values of approxi-

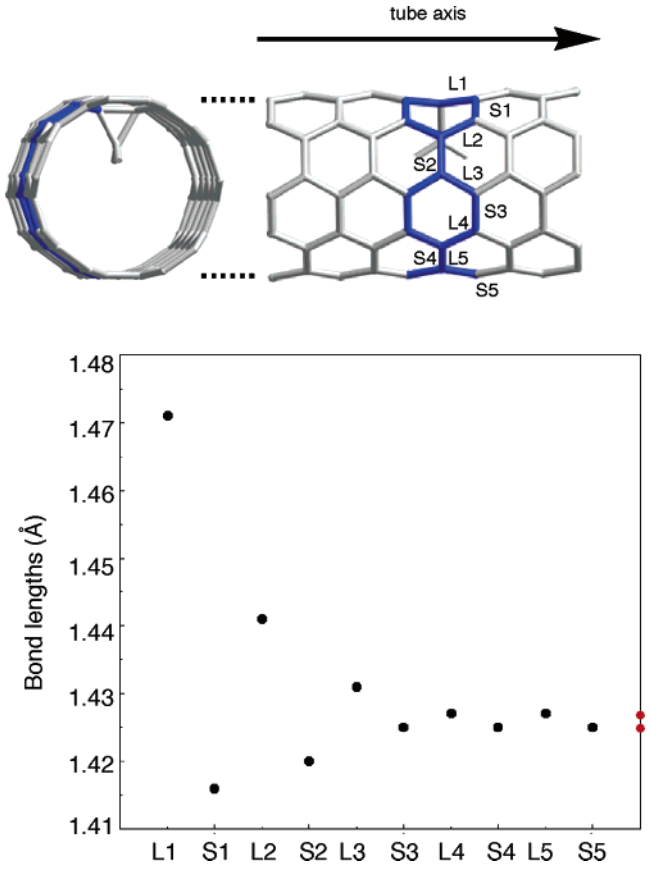

Figure 4. Bond distances in the circumferential direction of the optimized geometry **O** where the CH_2 molecule binds into the inner surface at an orthogonal (O) site as a function of S_n and L_n, where n is an integer. L and S represent long and short CC bonds, respectively. In the pristine (5,5) nanotube, the orthogonal CC bond is 1.427 Å long and the slanted CC bond is 1.423 Å long, both of which are given in red on the right.

Scheme 3

mately −160 and −130 kcal/mol, respectively, when the separations are larger than 6 Å. The energy difference between the orthogonal and slanted additions is ∼30 kcal/mol in this region, being similar to that of the first addition. When the separations are smaller than 6 Å, binding energies deviate from the constant values for both types of binding sites. In particular, the $O_2(0)$ site, which is nearest to the first binding site within the orthogonal sites, is the most stable. Within slanted sites, the nearest site $S_{0-1}(1)$ is the least stable, and the second nearest site $S_{1-2}(1)$ is the most stable.

To clarify the effects of the local modifications on the site preferences for the second addition, we define an interaction energy between the first and second CH_2 additions

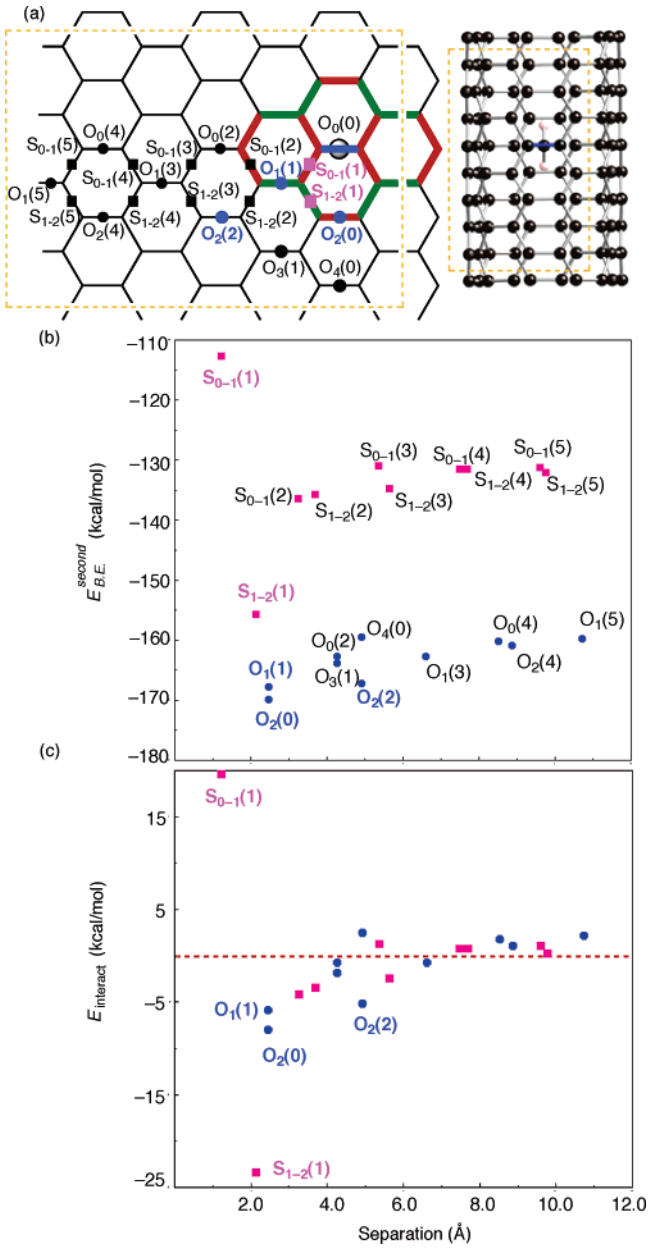

Figure 5. (a) Twenty sites for the binding of the second CH_2 molecules relative to the binding site for the first CH_2 molecule ($O_0(0)$). (b) Binding energies for the double CH_2 additions $E_{B.E.}^{second}$ as a function of separations of the two binding sites between the first and second attachment projected upon graphene. (c) Relationships between interaction energies $E_{interact}$ as a function of the separation between the first and second attachments. Orthogonal bindings are given by blue circles, and slanted bindings given by purple squares.

as $E_{interact}(X) = E_{B.E.}^{second}(X) - E_{B.E.}^{first-out}(X) - E_{B.E.}^{first-in}(O)$ in Figure 5b, where X represents binding sites **O** or **S** for the second CH_2 molecule. Here, $E_{B.E.}^{first-out}(X)$ and $E_{B.E.}^{first-in}(O)$ indicate the binding energies for the addition of the single outer and inner CH_2 molecule, respectively. When the interaction energy has a negative value, the local modifications, created by the first addition, should preferentially influence the second CH_2 molecule to bind at site X. Figure 5c shows that interaction energies become significant with decreasing separations between the first and second binding sites. The values converge to zero with increasing separations, as expected. However, there are cooperative effects for separations under 6 Å that might be used to do interesting

chemistry. With respect to the orthogonal bindings, the CH_2 bindings into the $O_2(0)$, $O_1(1)$, and $O_2(2)$ sites are significantly stabilized by the first addition. Within the $O_2(0)$, $O_1(1)$, and $O_2(2)$ sites, the stability is the highest for the $O_2(0)$ arrangement of the CH_2 molecule whose interaction energy is -7.9 kcal/mol, and energies decrease in absolute value in the order $O_2(0) > O_1(1) > O_2(1)$. The $O_2(0)$ and $O_1(1)$ sites correspond to CC bonds involved in the modified region colored by red and green in Figure 5a and the $O_2(1)$ site correspond to CC bonds nearest to the modified region, which points to the importance of local geometry changes created by the first addition. Although the slanted attachments are less stable than the orthogonal ones, the effects of the local geometry changes on slanted additions near the first binding site are also significant. The CH_2 molecule prefers the $S_{1-2}(1)$ site on the deformed SWNT surface by 24 kcal/mol relative to the unperturbed systems, whereas the binding into the $S_{0-1}(1)$ site is destabilized. The $S_{1-2}(1)$ and $S_{0-1}(1)$ sites correspond to CC bonds located in the bisnorcaradiene-like framework in Figure 5a. Because the significantly influenced binding sites $O_2(0)$, $O_1(1)$, $O_2(1)$, $S_{0-1}(1)$ and $S_{1-2}(1)$ are located in the bisnorcaradiene-like and quinonoid-like frameworks (Figure 5(a)), the local modifications of the surface should be responsible for their stabilities as well as site preferences for the CH_2 additions. Similar discussion can be applied to the finite-length $C_{140}H_{20}$ systems in Figure S2 (Supporting Information).

Conclusions

The PW91 DFT calculations show that the surface is modified in a larger region by covalent bond formation with an inner CH_2 molecule, compared to bond formation with an outer CH_2 molecule. Because of removal of two π-electrons, the π-network on the surface in the endohedral addition is disrupted to form the bisnorcaradiene-like framework in the axial direction and a quinonoid structure in the circumferential direction, whereas the π-network in the exohedral addition, where the number of π-electrons is unchanged, retains Clar structures of the pristine nanotube. The local modifications, created by the endohedral addition, influence the site-preferences for second CH_2 additions, and the effects are limited to the vicinity of the binding site. In fact, the binding of the second CH_2 that is most stable in energy is further stabilized by $\sim$8.0 kcal/mol by the local modification of the surface because of the endohedral addition. The interactions of the first CH_2 molecule with the inner surface can enhance site-selectivities for the second addition. Thus, we find cooperative behaviors in binding sites between the first and second CH_2 absorbents through the modifications of the surface of carbon nanotubes.

Acknowledgment. Support by the Japan Society for the Promotion of Science (JSPS) for a postdoctoral fellowship (T.Y.), computational support from the National Center for Supercomputing Applications (NCSA), and NSF Grant DMR-0331710 are gratefully acknowledged. We thank Prof. S. Iijima, Dr. K. Suenaga, and Dr. Y. Sato for valuable discussion on nanopeapods using TEM observations. We also thank Dr. K. Kamaras for calling our attention to refs 12 and 13.

Supporting Information Available: Potential energy along $d_{1,6}$ of 1,6-methano-[10]annulene at PW91PW91/6-31G* (Figure S1) and binding energy and interaction energy for the second CH_2 additions in the finite-length $C_{140}H_{20}$ nanotube (Figure S2); complete ref 23. This material is available free of charge via the Internet at http://pubs.acs.org.

CM0623108